International Journal of Chemistry, Mathematics and Physics (IJCMP)
[Vol-7, Issue-1, Jan-Feb, 2023]
https://dx.doi.org/10.22161/ijcmp.7.1.1
ISSN: 2456-866X

Structural, morphological, and photoluminescence study of Europium doped spinel $ZnAl_2O_4$ phosphors

N. M. Gahane1, P. J. Chaware[2,*], K. G. Rewatkar[3]

[1]Department of Physics, Hislop College, Nagpur, India
[2]Department of Physics, Dr. Ambedkar College, Nagpur, India
[3]Department of Physics, Vidya Vikas Mahavidyalay, Samudrapur, India
*Corresponding Author

Received: 03 Dec 2022; Received in revised form: 03 Jan 2023; Accepted: 10 Jan 2023; Available online: 18 Jan 2023

Abstract— *Nanocrystalline Eu-doped Zinc aluminate spinel was produced by a combustion method. Different methods, including X-ray diffraction (XRD), Scanning electron microscopy (SEM), Transmission electron microscopy (TEM), and photoluminescence spectroscopy, were used to examine the prepared spinel type $ZnAl_2O_4$ ceramic material and characterize its structural, morphological, and photoluminescent properties. The formation of a pure phase with a spinel structure and the space group $fd\bar{3}m$ is confirmed by the zinc aluminate material's X-ray diffraction pattern. Scan and transmission electron microscopy were used to further establish the average surface structure and crystalline size. The PL spectra show the strongest emission at 616 nm corresponds to the $^5D_0 \rightarrow {}^7F_2$ transition of Eu^{3+}. Photometric parameters like CIE coordinates and CCT values show that prepared phosphor that gives off a bright red light is used in the display and lamp industries.*

Keywords— ***photoluminescence, zinc aluminate, XRD, SEM, TEM, CIE.***

I. INTRODUCTION

Researchers have focused a lot of their effort recently on creating phosphors-converted LED chips activated by near UV and UV range in response to the growing need for solid-state lighting devices with high efficiency, high thermal stability, low cost, and energy-saving capabilities. Due to its numerous benefits, including their high luminous brightness, prolonged afterglow period, superior chemical stability, and environmental friendliness, rare-earth doped long-persistence materials have been extensively researched. The best rare-earth ion hosts are alkaline earth aluminates [1–5].

A well-known wide-bandgap semiconductor with strong optical and catalytic capabilities is zinc aluminate ($ZnAl_2O_4$). It's a naturally occurring mineral known as gahnite. A mixture of zinc and aluminum oxide, $ZnAl_2O_4$, has a spinel group crystal structure. Spinels have the generic formula AB_2O_4, where A and B stand for divalent and trivalent cations, respectively [6,7]. $ZnAl_2O_4$ is often used as a catalyst, in ceramics, and in electronics [8]. Several investigations have detected rare earth and transition metal in the $ZnAl_2O_4$ lattice. $ZnAl_2O_4$ was explored as a host lattice for trivalent rare-earth ions including Cr^{3+} [9], Sm^{3+} [10] and Ce[11]$^{3+}$, which generate visible light for display technologies.

Due to their high quantum efficiency, trivalent europium doped nano-size phosphor has been the subject of extensive study in recent years, making it a promising material for use in a wide range of devices and applications including light-emitting diodes (LEDs), white light-emitting diodes (WLEDs), photovoltaics, photocatalysts, display panels, and biometric sensors [12,13]. Eu^{3+} doped phosphors exhibit sharp, intense, and narrow emission spectra due to its $^5D_0 \rightarrow {}^7F_J$ (J = 0, 1, 2, 3, and 4) transitions under UV irradiation [14,15].

In this work, urea was used as the fuel to create $ZnAl_2O_4$ phosphors that were doped with Eu^{3+} using the combustion synthesis technique. XRD was used to evaluate phosphor phase purity and structure. SEM and TEM were used to analyse morphology. A fluorescence spectrophotometer measured photoluminescence at room temperature.

Nanophosphors' photoluminescent colour was calculated using the CIE chromaticity diagram.

II. EXPERIMENTAL

The $ZnAl_2O_4:Eu^{3+}$ phosphors were prepared using a auto-combustion method. Zinc nitrate [$Zn(NO_3)_24H_2O$], and aluminum nitrate nonahydrate[$Al(NO_3)_39H_2O$] were used as the oxidizers, while urea (CH_4N_2O) was used as the fuel for the method. Europium oxide (Eu_2O_3) was used as the dopant precursor. All reagents were of A.R. quality and were measured according to their stoichiometric ratio.

Fig.1 depicts a flowchart of the synthesis procedure. A mortar and pestle was used to mix the precursor and first reactant components in a china dish after they had been dissolved in double-distilled water. To create a homogeneous solution, the mixture was afterwards heated at 80 °C for 15-20 minutes. The solution boiled as soon as the china dish was placed in the preheated furnace (at 525 °C), starting a breakdown process. As a consequence, combustible gases including nitrogen oxides and ammonium oxides were released as a result of a combustion process. The process of combustion is completed fast. The resulting sample was frothy, and once the combustion process was finished, the foamy powder was collected. The foamy powder was finely ground before being sintered at 800 °C for four hours. A characterization process was applied to the finished product, and it was done at room temperature.

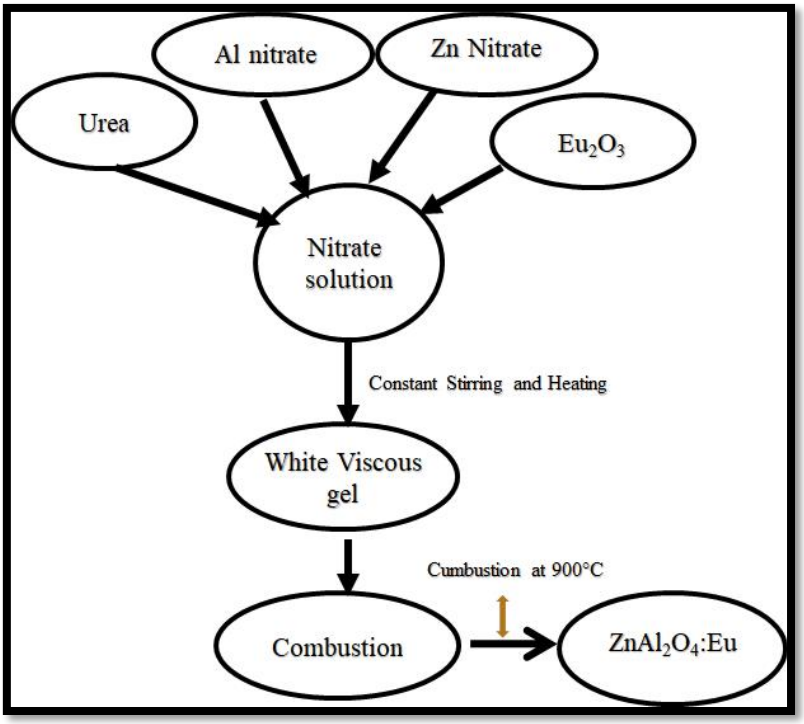

Fig.1 The schematic of the synthesis process $ZnAl_2O_4:2\%Eu^{3+}$

III. RESULTS AND DISCUSSION

X-RAY DIFFRACTION ANALYSIS

The XRD spectra of synthesized phosphors are analyzed in order to establish the phase purity, and crystallinity of the material. The obtained XRD spectra of 2% Eu-doped $ZnAl_2O_4$ are shown in **Fig.2**. All of the diffraction peaks can be precisely correlated to $ZnAl_2O_4$ with a face-centered cubic spinel structure. It is evident that the patterns match the typical $ZnAl_2O_4$ pattern for the space group Fd3m (JCPDS # 01-071-0968). The spinel structure that was previously reported agrees with all of the peaks [6,16]. The characteristic peaks at 2θ of 30.45°, 36.53°, 44.36°, 50.19°, 58.97°, and 64.71° are corresponding to (220), (311), (400), (331), (422), and (440) diffraction planes. Similar behaviour may be seen in the peaks and intensities of the synthetic powder and the standard. This shows that under the experimental conditions used in this study, the $ZnAl_2O_4$ spinel phase completely formed. Furthermore, there were no contaminants found in the synthesised sample. The the Scherrer equation [17] was used to determine the average crystallite size, which was approximately 25.854 nm.

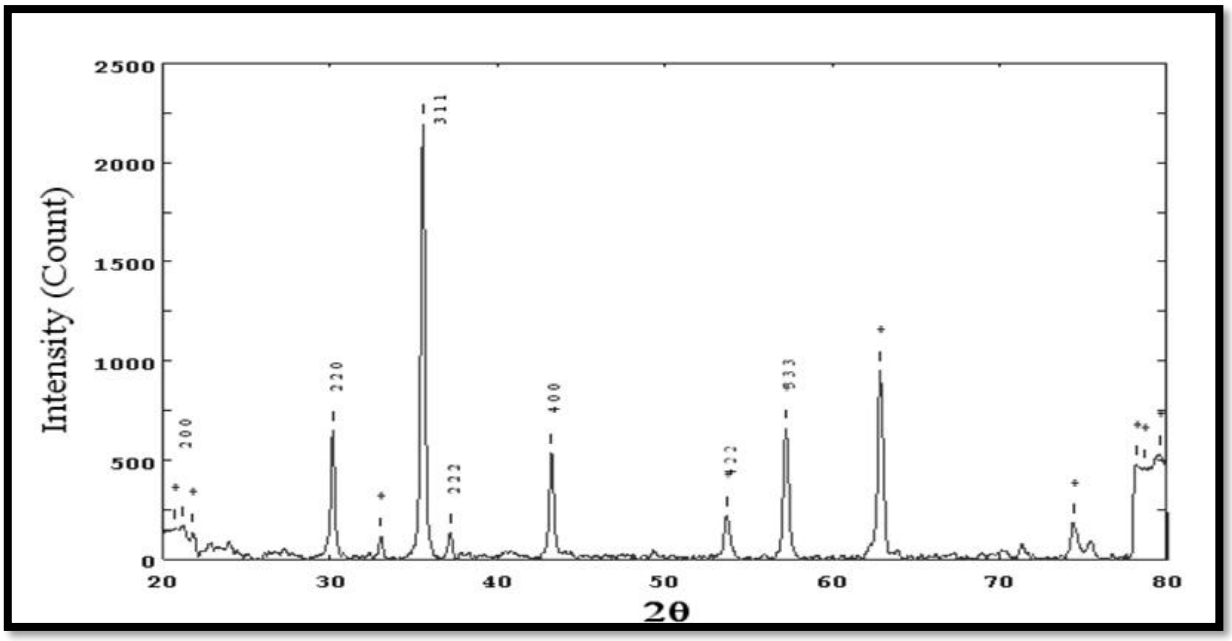

Fig.2 Thte XRD patterns $ZnAl_2O_4$:2%Eu^{3+}phosphor

Table 1 Various parameters, i.e. Lattice constants (a), cell volume (V), and crystallite size (D)

Sr. No.	Lattice Parameter (a) (A^0)	Cell Volume (A^0)	Bulk Density (D) gm/cm^3	X-Ray Density (Dx) gm/ cm^3	Porosity	Particle Size (nm)
1.	8.2444 A^0	560.372	2.1138	5.135	58.835	25.854

Morphological studies

The scanning electron microscopy (SEM) image from **Fig.3(a)** shows well-defined cubic morphology and narrow size distribution of the particle. The transmission electron microscopy (TEM) image from **Fig.3(b)** shows that the sample is composed of dispersed cubic particles with an average diameter of 70-80 nm which is compatible.

Crystallographic interpretation of the prepared sample was done in the reciprocal space by recording the Selected Area Electron Diffraction pattern (SAED) of the Eu doped $ZnAl_2O_4$ nano sample **Fig.3(c)**. A set of important Debye rings corresponding to hkl planes: 113 (d=2.623 Å), 004 (d=2.623 Å), 333 (d=2.623 Å) and 044 (d=2.623 Å) of the basic magnesium aluminate cubic crystal structure (space group: Fd3m). This further supports the fact that the sample is firmly in the nano-regime because the Debye rings looked to be continuous and dispersed.

PHOTOLUMINESCENCE

The **Fig.4** shows the excitation and emission spectra of $ZnAl_2O_4$: 2%Eu^{3+}. The 616 nm emission wavelength was used to monitor the excitation spectra, which had a wide band with a peak at around 465 nm that is attributed to transitions in the $^4f_6$ configuration of Eu^{3+} ions.

The visible emission spectrum of $ZnAl_2O_4$:2%Eu^{3+} under the excitation of 465nm, phosphor emits a narrow, intense emission band at 616 nm as well as multiple smaller emission bands. The main emission band should be recognized as the transition from splitting level $^5D_0 \rightarrow ^7F_2$ of Eu^{3+}. The emission spectra must be identified as the transitions $^5D_0 \rightarrow ^7F_j$. The spectra which are attributable to the transitions $^5D_0 \rightarrow ^7F_j$ consist of some bands according to the number of stark components of ^7F_j. The number of stark components of Eu^{3+} in $ZnAl_2O_4$ crystal follows the 2J+1 rule. The bands due to the transition $^5D_0 \rightarrow ^7F_1$ are 581, 588, 593, and 599 nm, transition $^5D_0 \rightarrow ^7F_2$ are 620 and 630 nm, and transition $^5D_0 \rightarrow ^7F_3$ are 650 and 658 nm [18–21]. The hypersensitive band at 615 nm can be associated with the electric dipole transition $^5D_0 \rightarrow ^7F_2$ of Eu^{3+} ions.

The CIE chromaticity diagram of $ZnAl_2O_4$:2%Eu^{3+} phosphors is shown in **Fig.5**. The CIE coordinates (0.5724,

0.4267) indicate red emission with a CCT of 1748 K and a CRI of 42. The CIE values of $ZnAl_2O_4$:2%Eu^{3+} red phosphor are nearly identical to those of the commercial red-emitting phosphor Y_2O_3:Eu^{3+} [22,23].

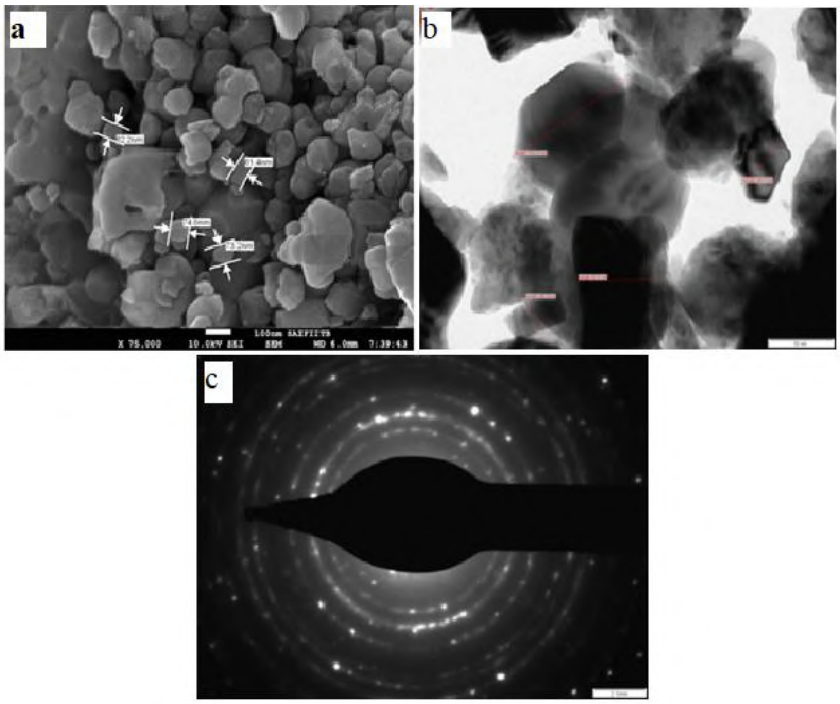

Fig.3 (a) The SEM (b) the TEM and (c) SAED images of $ZnAl_2O_4$:2%Eu^{3+} powder

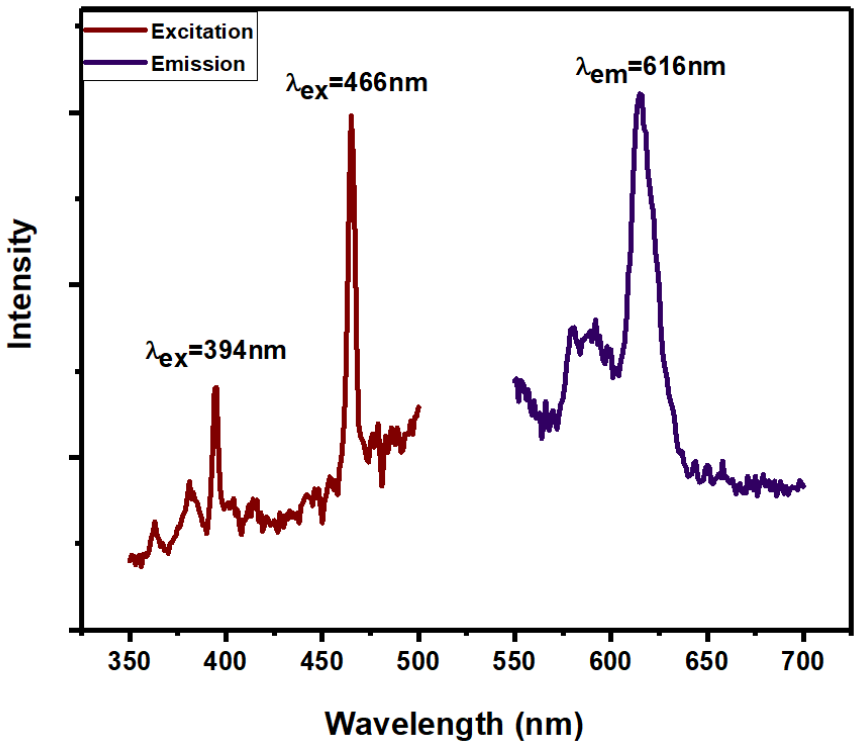

Fig.4 Photoluminescence graph of $ZnAl_2O_4$:2%Eu^{3+} Phosphor

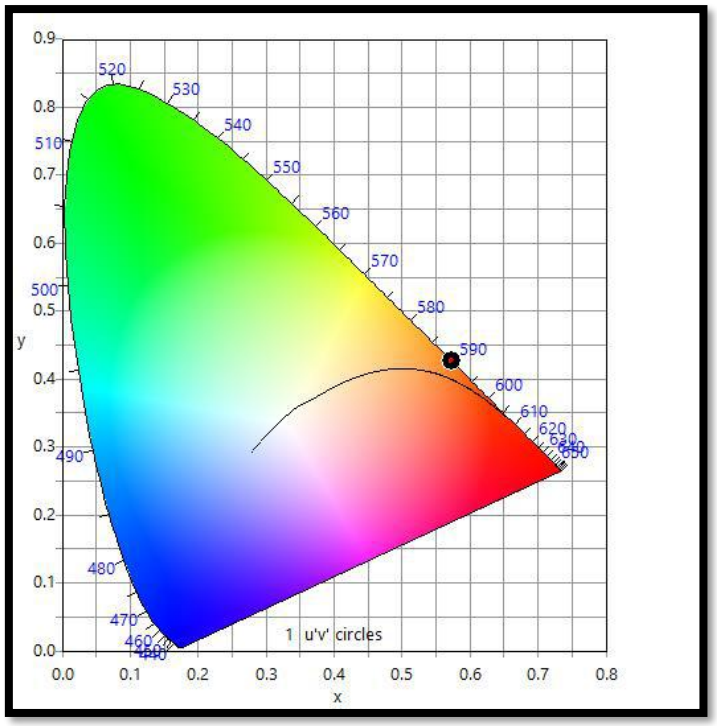

Fig.5 The CIE chromaticity diagram of $ZnAl_2O_4$:2%Eu^{3+} phosphors

IV. CONCLUSION

Our results show that Eu is kept in the trivalent oxidation state in the produced $ZnAl_2O_4$ phosphor. With the combustion process, this phosphor could be made in a short amount of time, which would slow down the rate of aluminate synthesis. XRD patterns showed that Eu-doped Zinc aluminate samples were made of cubic spinel nanoparticles, and the Debye-Scherrer formula showed that the grain size was 25.45 nm. The SEM image shows that the particle has a clear cubic shape and a narrow range of sizes. TEM images indicate distributed cubic particles with an average diameter of 70-80 nm, which is compatible. According to the PL spectrum, the Eu^{3+} ion's $^5D_0 \rightarrow {}^7F_2$ transition results in the maximum emission at 616 nm, which corresponds to a brilliant red colour producing phosphor utilised in displays and lamp production. The red emission with a CCT of 1748 K and a CRI of 42 is shown by the CIE coordinates (0.5724, 0.4267).

REFERENCES

[1] P. Chaware, K.G. Rewatkar, Structural and photoluminescence study of $SrAl_2O_4$:Eu^{3+} phosphors synthesized by combustion method, International Journal of Chemistry, Mathematics and Physics (IJCMP). 5 (2021) 1–6. https://doi.org/10.22161/ijcmp.5.6.1.

[2] P.J. Chaware, Y.D. Choudhari, D.M. Borikar, K.G. Rewatkar, Photoluminescence and Judd-Ofelt analysis of Eu^{3+} doped akermanite silicate phosphors for solid state lighting, Opt Mater (Amst). 133 (2022). https://doi.org/10.1016/j.optmat.2022.112945.

[3] V.B. Pawade, H.C. Swart, S.J. Dhoble, Review of rare earth activated blue emission phosphors prepared by combustion synthesis, Renewable and Sustainable Energy Reviews. 52 (2015) 596–612. https://doi.org/10.1016/j.rser.2015.07.170.

[4] V.B. Bhatkar, N. v. Bhatkar, Combustion synthesis and photoluminescence study of silicate biomaterials, Bulletin of Materials Science. 34 (2011) 1281–1284. https://doi.org/10.1007/s12034-011-0166-5.

[5] T. Peng, H. Yang, X. Pu, B. Hu, Z. Jiang, C. Yan, Combustion synthesis and photoluminescence of SrAl2O 4:Eu,Dy phosphor nanoparticles, Mater Lett. 58 (2004) 352–356. https://doi.org/10.1016/S0167-577X(03)00499-3.

[6] R. Priya, A. Negi, S. Singla, O.P. Pandey, Luminescent studies of Eu doped $ZnAl_2O_4$ spinels synthesized by low-temperature combustion route, Optik (Stuttg). 204 (2020) 164173. https://doi.org/10.1016/j.ijleo.2020.164173.

[7] S. v. Motloung, M. Tsega, F.B. Dejene, H.C. Swart, O.M. Ntwaeaborwa, L.F. Koao, T.E. Motaung, M.J. Hato, Effect of annealing temperature on structural and optical properties of $ZnAl_2O_4$:1.5% Pb2+ nanocrystals synthesized via sol-gel reaction, J Alloys Compd. 677 (2016) 72–79. https://doi.org/10.1016/j.jallcom.2016.03.170.

[8] H. Zhao, Y. Dong, P. Jiang, G. Wang, J. Zhang, C. Zhang, $ZnAl_2O_4$ as a novel high-surface-area ozonation catalyst: One-step green synthesis, catalytic performance and mechanism, Chemical Engineering Journal. 260 (2015) 623–630. https://doi.org/10.1016/j.cej.2014.09.034.

[9] D. Zhang, Y.H. Qiu, Y.R. Xie, X.C. Zhou, Q.R. Wang, Q. Shi, S.H. Li, W.J. Wang, The improvement of structure and photoluminescence properties of $ZnAl_2O_4$:Cr^{3+} ceramics

synthesized by using solvothermal method, Mater Des. 115 (2017) 37–45. https://doi.org/10.1016/j.matdes.2016.11.034.

[10] S.P. Khambule, S. v. Motloung, T.E. Motaung, L.F. Koao, R.E. Kroon, M.A. Malimabe, Tuneable blue to orange phosphor from Sm^{3+} doped $ZnAl_2O_4$ nanomaterials, Results in Optics. 9 (2022). https://doi.org/10.1016/j.rio.2022.100280.

[11] B.S. Ravikumar, H. Nagabhushana, S.C. Sharma, B.M. Nagabhushana, Low temperature synthesis, structural and dosimetric characterization of $ZnAl_2O_4:Ce^{3+}$ nanophosphor, Spectrochim Acta A Mol Biomol Spectrosc. 122 (2014) 489–498. https://doi.org/10.1016/j.saa.2013.10.106.

[12] P. Halappa, S.T. Raj, R. Sairani, S. Joshi, R. Madhusudhana, C. Shivakumara, Combustion synthesis and characterisation of Eu^{3+}-activated Y2O3red nanophosphors for display device applications, Int J Nanotechnol. 14 (2017) 833–844. https://doi.org/10.1504/IJNT.2017.086767.

[13] K. Mori, H. Onoda, T. Toyama, N. Osaka, Y. Kojima, Synthesis and fluorescence studies of Eu^{3+}-doped SrAl12O19 phosphor, Optik (Stuttg). 180 (2019) 183–188. https://doi.org/10.1016/j.ijleo.2018.11.047.

[14] I.E. Kolesnikov, E. v. Golyeva, E.V. Borisov, E.Y. Kolesnikov, Photoluminescence properties of Eu^{3+}-doped MgAl2O4 nanoparticles in various surrounding media, ChemInform. 40 (2009) 806–811. https://doi.org/10.1016/j.jre.2018.10.019.

[15] V. Sivakumar, U. v. Varadaraju, Synthesis, phase transition and photoluminescence studies on Eu^{3+}-substituted double perovskites-A novel orange-red phosphor for solid-state lighting, J Solid State Chem. 181 (2008) 3344–3351. https://doi.org/10.1016/j.jssc.2008.08.030.

[16] S. v. Motloung, F.B. Dejene, H.C. Swart, O.M. Ntwaeaborwa, Effects of Zn/citric acid mole fraction on the structure and luminescence properties of the un-doped and 1.5% Pb2+ doped $ZnAl_2O_4$ powders synthesized by citrate sol-gel method, J Lumin. 163 (2015) 8–16. https://doi.org/10.1016/j.jlumin.2015.02.027.

[17] Y.D. Choudhari, K.G. Rewatkar, Influence of Bi^{3+} ions substitution on structural, magnetic, and electrical properties of lead hexaferrite, J Magn Magn Mater. 551 (2022) 169162. https://doi.org/10.1016/J.JMMM.2022.169162.

[18] R. v. Perrella, C.S. Nascimento, M.S. Góes, E. Pecoraro, M.A. Schiavon, C.O. Paiva-Santos, H. Lima, M.A. Couto Dos Santos, S.J.L. Ribeiro, J.L. Ferrari, Structural, electronic and photoluminescence properties of Eu^{3+}-doped CaYAlO4 obtained by using citric acid complexes as precursors, Opt Mater (Amst). 57 (2016) 45–55. https://doi.org/10.1016/j.optmat.2016.04.012.

[19] A. Azhagiri, V. Ponnusamy, R. Satheesh Kumar, A development of new red phosphor based on europium doped as well as substituted Barium Lanthanum Aluminate (BaLaAlO4: Eu^{3+}), Opt Mater (Amst). 90 (2019) 127–138. https://doi.org/10.1016/j.optmat.2019.02.024.

[20] D.S. Bobade, P.B. Undre, Synthesis and Luminescence Properties of Eu^{3+} Doped Sr2SiO4 Phosphor, Integrated Ferroelectrics. 205 (2020) 72–80. https://doi.org/10.1080/10584587.2019.1675001.

[21] P. Chaware, A. Nande, S.J. Dhoble, K.G. Rewatkar, Structural, photoluminescence and Judd-Ofelt analysis of red-emitting Eu^{3+} doped strontium hexa-aluminate nanophosphors for lighting application, Opt Mater (Amst). 121 (2021) 111542. https://doi.org/10.1016/j.optmat.2021.111542.

[22] C.S. McCamy, Correlated color temperature as an explicit function of chromaticity coordinates, Color Res Appl. 17 (1992) 142–144. https://doi.org/10.1002/col.5080170211.

[23] X. Huang, Q. Sun, B. Devakumar, Preparation, crystal structure, and photoluminescence properties of high-brightness red-emitting $Ca_2LuNbO_6:Eu^{3+}$ double-perovskite phosphors for high-CRI warm-white LEDs, J Lumin. 225 (2020) 117373. https://doi.org/10.1016/j.jlumin.2020.117373.